Edge Strength Similarity for Image Quality Assessment

Xuande Zhang, Xiangchu Feng, Weiwei Wang, and Wufeng Xue

***Abstract*—The objective image quality assessment aims to model the perceptual fidelity of semantic information between two images. In this letter, we assume that the semantic information of images is fully represented by edge-strength of each pixel and propose an edge-strength-similarity-based image quality metric (ESSIM). Through investigating the characteristics of the edge in images, we define the edge-strength to take both anisotropic regularity and irregularity of the edge into account. The proposed ESSIM is considerably simple, however, it can achieve slightly better performance than the state-of-the-art image quality metrics as evaluated on six subject-rated image databases.**

***Index Terms*—Edge-strength, image quality assessment, regularity and irregularity.**

I. Introduction

In recent years, there has been extensive interest in developing objective image quality assessment (IQA) metrics. Such metrics have wide applications in the field of computer vision and image processing [1]. According to the availability of the ground-truth images in the assessment process, they can be classified into full-reference (FR), reduced-reference (RR) and no-reference (NR) metrics. In this letter, the discussion is confined to FR metrics, where the ground-truth images are available and known as the reference images.

The L2-fidelity related IQA metrics, such as signal to noise ratio (SNR) and peak SNR (PSNR), are most widely used in image processing. But these metrics do not consider the properties of human visual system (HVS) and show poor consistency with subjective evaluations. Since the introduction of structural similarity index (SSIM) [1], a flood of IQA metrics have been developed with attempt to achieve high consistency with subjective assessment [2]–[7]. The SSIM assumed that the HVS is highly adapted for extracting structural information from a scene and the local structure similarity reflects the visual fidelity well. In [6], Zhang. *et al.* proposed a feature similarity index for image quality assessment (FSIM), this metric evaluated the visual fidelity in the both phase congruency and gradient feature space with the assumption that the HVS perceives images according to low-level features. A thorough comparison of the performance between FSIM and other representative IQA metrics are presented in [7], which indicated that FSIM achieves the best assessment performance so far.

An ideal IQA metric should perfectly mimic the HVS. Unfortunately, the HVS itself is not well understood until now. As a consequence, most existing IQA metrics are only designed on the basis of certain assumption about the HVS. An apparent fact is that human semantically perceive the image and evaluate the quality of the image based on the distortion of semantic information. Consider the simple example of locally adding the same amount of noise to a face image, it is obvious that the manipulating region is deterministic for the quality of the resulting image. If the hair region is contaminated, the resulting face image still looks quite perfect. But, if the semantically significant region, such as that of eyes, nose or the lips, is contaminated, the resulting image would look very unpleasant and would receive a low subjective quality score. This example verifies that the human rates the image quality according to the distortion of semantic information. However, accurately measuring the semantic information remains a very challenging task.

In this letter, we assume that the semantic information of images is mainly represented by the edge-strength of each pixel, the edge-strength quantifies the chance or possibility of a pixel belonging to the edge of a semantic object. We will analyze the characteristics of semantic edge and define the edge-strength to follow these characteristics, and then we propose an image quality metric based on the edge-strength similarity. The proposed metric is conceptually very simple and can be implemented with very low complexity. However, it leads to promising assessment performance as evaluated on the publically available data sets.

II. Edge-Strength Similarity Based Image Quality Metric

A. Three Characteristics of the Edge and the Definition of Edge-Strength

The edge is a fundamental concept in computer vision, particularly in the area of object extraction and image segmentation. Ideally, the edge is a set of pixels indicating the boundary of semantic objects in the image. In practice, it is always identified by collecting the set of pixels at which the image changes sharply, or has discontinuity. However, discontinuity is only one side of

Manuscript received October 11, 2012; revised December 14, 2012; accepted January 15, 2013. Date of publication January 30, 2013; date of current version February 15, 2013. This work was supported by the National Science Foundation of China (Grants 61001156, 61105011, 11101292, 60872138 and 61271294) and by the National Science Foundation of Ningxia University (ZR1206). The associate editor coordinating the review of this manuscript and approving it for publication was Prof. Weisi Lin.

X. Zhang is with Department of Applied Mathematics, School of Science, Xidian University, Xi'an, China and also with School of Mathematics and Computer Science, Ningxia University, Yinchuan, China (e-mail: love_truth@126.com).

X. Feng and W. Wang are with Department of Applied Mathematics, School of Science, Xidian University, Xi'an, China (e-mail: xcfeng@mail.xidian.edu.cn; wwwang@mail.xidian.edu.cn).

W. Xue is with Institute of Image Processing and Pattern Recognition, Xi'an Jiaotong University, Xi'an, China (e-mail: x.wolfs@stu.xjt.edu.cn).

Color versions of one or more of the figures in this paper are available online at http://ieeexplore.ieee.org.

Digital Object Identifier 10.1109/LSP.2013.2244081

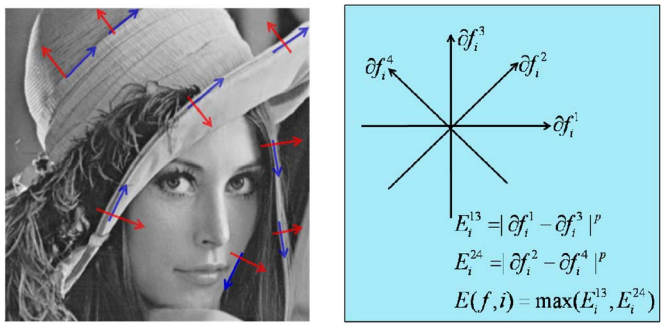

(a) (b)

Fig. 1. (a) Characteristics of the edge: the regularity along certain direction (blue arrow), the irregularity along its orthogonal direction (red arrow), the edge may stretch out in multiple directions. (b) The directional derivatives considered in this study and the definition of the edge-strength.

the coin about the edge. Even an at-a-glance investigation can reveal that the edges at least have three characteristics as shown in Fig. 1(a).

(c1). The local regularity/smoothness/continuity along certain direction.

(c2). The local irregularity/oscillation/discontinuity along the orthogonal direction.

(c3). There exists anisotropic structures in the image and the edges always stretch out in multiple directions.

It is the unification of (c1) and (c2) that makes the semantic meaningful edges possible, the constant image and the pure noise image are two extreme instances for which merely (c1) or (c2) is satisfied, and we cannot find any edges in these two special images. These coupled characteristics of the edge have been early considered in image restoration. In [8] Perona and Malik (P-M) proposed an inhomogeneous model to smooth along the edges and simultaneously to avoid the smoothing across edges for structure-preserving image denoising. Motivated by the success of P-M model, we define the edge-strength to take all the above three characteristics into account.

Denote the reference image as

$$f = [f_1, \cdots, f_i, \cdots, f_N] \in R^N,$$

where i indexes the pixels and N denotes the total number of pixels. The local regularity of the image along multiple directions is measured by directional derivatives, let ∂f_i^j denote the directional derivative at the ith pixel along the direction indexed by j. In this study, we only consider four directions as illustrated in Fig. 1(b) for simplicity, namely, $j = 1, 2, 3, 4$. It should be noted that the regularity along a direction and the irregularity along its orthogonal direction together imply the possibility of an edge, which means the difference between the regularity/varying trends along two orthogonal directions give the likelihood of the edge. Then, we define the edge-strength in the diagonal directions as

$$E_i^{2,4}(f) = \left|\partial f_i^2 - \partial f_i^4\right|^p, \tag{1}$$

where p is introduced to nonlinearly rescale the edge-strength to fit the human perception. Similarly, the edge-strength in the vertical or horizontal direction is defined as

$$E_i^{1,3}(f) = \left|\partial f_i^1 - \partial f_i^3\right|^p. \tag{2}$$

Since the HVS is more sensitive to the direction showing stronger edge-strength, we define the total edge-strength around the ith pixel as

$$E(f,i) = \max\left(E_i^{1,3}(f), E_i^{2,4}(f)\right). \tag{3}$$

This newly defined edge-strength has taken all the three characteristics of the edge into account and can be easily computed through convolution.

Denote the distorted image of f as

$$g = [g_1, \cdots, g_i, \cdots, g_N] \in R^N.$$

To ensure that the edge-strength of f and g at each pixel can be compared in the same direction, we define the edge-strength of g at the i th pixel as

$$E(g,i) = \begin{cases} E_i^{1,3}(g) & \text{if } E(f,i) = E_i^{1,3}(f) \\ E_i^{2,4}(g) & \text{if } E(f,i) = E_i^{2,4}(f) \end{cases}, \tag{4}$$

where $E_i^{1,3}(g)$ and $E_i^{2,4}(g)$ are defined in the same form of (1) and (2).

Note that any directional high-pass filters can be used to define the edge-strength, we employ the directional derivatives here for simplicity. Additionally, the directional derivatives ∂f_i^j, $i = 1, 2, \cdots N$ are computed by convolving the image f with the kernels K^j, $j = 1, 2, 3, 4$ which take the following form:

$$K^1 = \frac{1}{16}\begin{bmatrix} 0 & 0 & 0 & 0 & 0 \\ 0 & -3 & 0 & 3 & 0 \\ 0 & -10 & 0 & 10 & 0 \\ 0 & -3 & 0 & 3 & 0 \\ 0 & 0 & 0 & 0 & 0 \end{bmatrix}, \quad K^2 = \frac{1}{16}\begin{bmatrix} 0 & 0 & 3 & 0 & 0 \\ 0 & 0 & 0 & 10 & 0 \\ -3 & 0 & 0 & 0 & 3 \\ 0 & -10 & 0 & 0 & 0 \\ 0 & 0 & -3 & 0 & 0 \end{bmatrix},$$

$$K^3 = \frac{1}{16}\begin{bmatrix} 0 & 0 & 0 & 0 & 0 \\ 0 & 3 & 10 & 3 & 0 \\ 0 & 0 & 0 & 0 & 0 \\ 0 & -3 & -10 & -3 & 0 \\ 0 & 0 & 0 & 0 & 0 \end{bmatrix}, \quad K^4 = \frac{1}{16}\begin{bmatrix} 0 & 0 & 3 & 0 & 0 \\ 0 & 10 & 0 & 0 & 0 \\ 3 & 0 & 0 & 0 & -3 \\ 0 & 0 & 0 & -10 & 0 \\ 0 & 0 & -3 & 0 & 0 \end{bmatrix}.$$

Generally, different kernels can be used to compute the directional derivatives. The design or choice of kernels is quite important in IQA study, and different kernels may lead to different assessment performance. In [6] the authors compared three image gradient kernels (Prewitt [19], Sobel [19] and Scharr [20]) for their IQA algorithm. The comparison indicated that Scharr operator can lead to best performance. The above kernels K^j, $j = 1, 2, 3, 4$ are just designed based on Scharr operator.

B. Edge-Strength Similarity Based Image Quality Metric (ESSIM)

With edge-strength defined, the visual fidelity between f and g can be predicted by the similarity between their edge-strength maps. Specifically, the ESSIM index is defined as

$$ESSIM(f,g) = \frac{1}{N}\sum_{i=1}^{N}\frac{2E(f,i)E(g,i) + C}{(E(f,i))^2 + (E(g,i))^2 + C}, \tag{5}$$

where the parameter C has two senses. Firstly, it is introduced to avoid the denominator to be zero. Secondly, it can be viewed

TABLE I
THE PREDICTION PERFORMANCE OF TEN IQA METRICS, THE FIRST TWO BEST RESULTS ARE HIGHLIGHTED

		PSNR	IFC	VIF	VSNR	SSIM	MS-SSIM	IW-SSIM	GSM	FSIM	ESSIM
TID2008	SROCC	0.5245	0.5692	0.7496	0.7046	0.7749	0.8528	0.8559	0.8554	**0.8805**	**0.8843**
	KROCC	0.3696	0.4261	0.5863	0.5340	0.5768	0.6543	0.6636	0.6651	**0.6946**	**0.7049**
CSIQ	SROCC	0.8057	0.7482	0.9193	0.8106	0.8756	0.9138	0.9213	0.9126	**0.9242**	**0.9326**
	KROCC	0.6080	0.5740	0.7534	0.6247	0.6907	0.7397	0.7529	0.7403	**0.7567**	**0.7686**
LIVE	SROCC	0.8755	0.9234	**0.9631**	0.9274	0.9479	0.9445	0.9567	0.9554	**0.9634**	0.9622
	KROCC	0.6864	0.7540	0.827	0.7616	0.7963	0.7922	0.8175	0.8131	**0.8337**	**0.8397**
IVC	SROCC	0.6885	0.8978	0.8966	0.7983	0.9018	0.8847	0.9125	**0.9294**	**0.9262**	0.9239
	KROCC	0.5220	0.7192	0.7165	0.6036	0.7223	0.7012	0.7339	**0.7626**	0.7564	**0.7622**
MICT	SROCC	0.6130	0.8387	0.9086	0.8614	0.8794	0.8864	0.9202	**0.9233**	0.9059	**0.9251**
	KROCC	0.4447	0.6413	0.7329	0.6762	0.6639	0.7029	0.7537	**0.7541**	0.7302	**0.7588**
A57	SROCC	0.6189	0.3185	0.6223	**0.9355**	0.8066	0.8394	0.8709	0.9002	**0.9181**	0.9013
	KROCC	0.4309	0.2378	0.4589	**0.8031**	0.6058	0.6478	0.6842	0.7205	**0.7639**	0.7317

TABLE II
THE SROCC VALUE OF TEN IQA METRICS FOR EACH DISTORTION TYPE, THE FIRST TWO BEST RESULTS ARE HIGHLIGHTED

		PSNR	IFC	VIF	VSNR	SSIM	MS-SSIM	IW-SSIM	GSM	FSIM	ESSIM
TID2008	Awgn	**0.9070**	0.5806	0.8797	0.7728	0.8107	0.8086	0.7869	0.8576	0.8566	**0.8859**
	Awgn-color	**0.8995**	0.5460	**0.8757**	0.7793	0.8029	0.8054	0.7920	0.8077	0.8527	0.8134
	Spatial corr-noise	**0.9170**	0.5958	0.8698	0.7665	0.8144	0.8209	0.7714	0.8935	0.8483	**0.9130**
	Masked noise	**0.8515**	0.6732	**0.8683**	0.7295	0.7795	0.8107	0.8087	0.7468	0.8021	0.7523
	High-fre-noise	**0.9270**	0.7318	0.9075	0.8811	0.8729	0.8694	0.8662	0.8942	**0.9093**	0.9089
	Impulse noise	**0.8724**	0.5345	**0.8327**	0.6471	0.6732	0.6907	0.6465	0.7216	0.7452	0.7864
	Quantization noise	**0.8696**	0.5857	0.7970	0.8270	0.8531	0.8589	0.8177	**0.8790**	0.8564	0.8597
	Blur	0.8697	0.8559	0.9540	0.9330	0.9544	0.9563	**0.9636**	0.9603	0.9472	**0.9629**
	Denoising	0.9416	0.7973	0.9161	0.9286	0.9530	0.9582	0.9473	**0.9724**	0.9603	**0.9713**
	Jpg-comp	0.8717	0.8180	0.9168	0.9174	0.9252	0.9322	0.9184	**0.9391**	0.9279	**0.9436**
	Jpg2k-comp	0.8132	0.9437	0.9709	0.9515	0.9625	0.9700	0.9738	**0.9758**	**0.9773**	**0.9758**
	Jpg-trans-error	0.7516	0.7909	0.8585	0.8055	0.8678	0.8681	0.8588	**0.8790**	**0.8708**	0.8624
	Jpg2k-trans-error	0.8309	0.7301	0.8501	0.7909	0.8577	0.8606	0.8203	**0.8938**	0.8544	**0.8791**
	Pattern noise	0.5815	**0.8418**	0.7619	0.5716	0.7107	0.7377	**0.7724**	0.7382	0.7491	0.7180
	Block distortion	0.6193	0.6770	0.8324	0.1926	0.8462	0.7546	0.7623	**0.8858**	0.8492	**0.8881**
	Mean shift	0.6957	0.4250	0.5096	0.3715	**0.7231**	**0.7336**	0.7067	0.7206	0.6720	0.6685
	Contrast	0.5859	0.1713	**0.8188**	0.4239	0.5246	0.6381	0.6301	**0.6703**	0.6481	0.6454
CSIQ	Awgn	0.9363	0.8431	**0.9575**	0.9241	0.8974	0.9471	0.9380	0.9312	0.9262	**0.9494**
	Jpeg-comp	0.8881	0.9412	**0.9705**	0.9036	0.9546	0.9634	**0.9662**	0.9074	0.9654	0.9649
	Jpeg2k-comp	0.9362	0.9252	0.9672	0.9480	0.9606	**0.9683**	**0.9683**	0.9116	**0.9685**	0.9676
	Fnoise	0.9339	0.8261	**0.9511**	0.9084	0.8922	0.9331	0.9059	0.9154	0.9234	**0.9433**
	Blur	0.9291	0.9527	**0.9745**	0.9446	0.9609	0.9711	**0.9782**	0.8943	0.9729	0.9629
	Contrast	0.8621	0.4873	0.9345	0.8700	0.7922	0.9526	**0.9539**	0.8933	**0.9420**	0.9399
LIVE2	Jpeg2k-comp	0.8954	0.9113	0.9696	0.9551	0.9614	0.9627	0.9649	**0.9830**	0.9717	**0.9809**
	Jpeg-comp	0.8809	0.9468	**0.9846**	0.9657	0.9764	0.9815	0.9808	0.9793	**0.9834**	0.9819
	Awgn	**0.9854**	0.9382	**0.9858**	0.9785	0.9694	0.9733	0.9667	0.9725	0.9652	0.9764
	Gblur	0.7823	0.9584	0.9728	0.9413	0.9517	0.9542	0.9720	**0.9876**	0.9708	**0.9917**
	Fastfading	0.8907	**0.9629**	**0.9650**	0.9027	0.9556	0.9471	0.9442	0.9515	0.9499	0.9476

as a scaling parameter, the different magnitude of C will lead to the different ESSIM score. Here, we choose

$$C = (BL)^2,$$

in which B is a predefined constant, L is the dynamic range of the edge-strength. For the 8-bit grayscale images, the edge strength $E(f,i)$ satisfies $0 \leq E(f,i) \leq 255^p$, namely, $L = 255^p$. Then we have

$$C = (BL)^2 = (B255^p)^2 = \left(B^{\frac{1}{p}}255\right)^{2p} = (B_1 255)^{2p} \quad (6)$$

with $B_1 = B^{\frac{1}{p}}$.

There are overall two parameters need to be trained in order to calculate the ESSIM index (the nonlinear rescaling parameter p in (1) and the constant B_1 in (6)). The ESSIM index defined here is closely related with the gradient based methods [6], [9], [10]. In fact, the gradient itself can be viewed as the edge-strength measure, but the gradient is only responsible for the local variance along vertical and the horizontal direction and therefore cannot capture the anisotropic edges effectively. Additionally, the gradient does not explicitly consider the coupled characteristics (regularity and irregularity) of the edge discussed in the previous subsection.

III. EXPERIMENT RESULTS

A. Experiment Setup

The performance of the IQA metrics is evaluated by the consistency between the objective scores provided by the IQA metrics and the subjective mean opinion scores (MOSs). This consistency is measured by Spearman rank-order correlation coefficient (SROCC) and Kendall rank-order correlation coefficient (KROCC). We evaluate the proposed ESSIM on six publically available subject-rated image databases constructed for the evaluation of IQA algorithms, including TID2008 [11], CSIQ [12], LIVE2 [13], Image and Video Communication Database (IVC) [14], Media Information and Communication Technology Database (MICT) [15], and Cornell-A57 Database (A57) [16]. Due to the space limitation, we only choose nine representative IQA metrics, including PSNR, IFC [4], VIF [5], VSNR [2], SSIM [1], MS-SSIM [3], IW-SSIM [17], FSIM [6] and the gradient similarity based metric (GSM) [9],

for comparison. To guarantee a fair comparison, we use the "original" parameters configured by their authors for these nine metrics. For ESSIM, we tune the parameters on the subset of TID2008 composed of the first five reference images and the corresponding $17 \times 4 \times 5$ distorted images. Specifically, we search for the parameters on the two dimensional grids (p, B_1) for $p = 0.25m$, $B_1 = 5n$ with

$$m = -10, \cdots, -2, -1, 0, 1, 2, \cdots, 10; \quad n = 1, 2, \cdots 10$$

and finally set the parameters as the pair leading to the highest SROCC. As a result, we have $p = 0.5$, $B_1 = 10$. For color images, we only apply each IQA metric on the luminance component. The luminance component is extracted from RGB color image through

$$l = 0.299r + 0.587g + 0.114b,$$

where r, g, b is respectively the R,G, B component and l is the luminance component. All these IQA metrics are implemented in Matlab and executed on the DELL D630 PC (Dual core 2.1 GHz CPU and 2 G RAM). The Matlab code accompanying the current work is available on http://www.mathworks.com/matlabcentral/fileexchange/authors/96116.

B. Performance Comparison

The prediction performance of all 10 IQA metrics over six databases is listed in Table I, which illustrates that the ESSIM slightly outperforms the FSIM. Additionally, these comparisons indicate that the proposed ESSIM averagely outperforms the gradient based method [9]. Since the gradient only considers the average changes/regularity of the image at each pixel and does not simultaneously take the three characteristics of the edge into account, then these comparisons partly verify the usefulness of the three characteristics of the edge.

To provide a distortion-specific comparison among these IQA metrics, we compute the SROCC coefficients of each metric for each distortion type. The three largest datasets, TID2008 [11], CSIQ [12] and LIVE2 [13], are employed in this comparison. The results are listed in Table II, from which we can observe that the proposed ESSIM index performs quite well on the type of distortion which leads to significant edge-strength changes, such as "Gblur" in LIVE2 and "Block distortion" in TID2008.

IV. Conclusion

This letter presents a FR IQA metric based on the edge-strength similarity, which complementally exploits the anisotropic regularity and irregularity of the edges presented in images. The experiment results on the subject-rated image databases indicate that the proposed metric is quite competitive in terms of both assessment performance and computational complexity.

Acknowledgment

The authors sincerely appreciate Dr.Jieying Zhu and the authors of [6] for insightful discussions.

References

[1] Z. Wang, A. C. Bovik, H. R. Sheikh, and E. P. Simoncelli, "Image quality assessment: From error visibility to structural similarity," *IEEE Trans. Image Process.*, vol. 13, no. 4, pp. 600–612, Apr. 2004.

[2] M. Chandler and S. S. Hemami, "VSNR: A wavelet-based visual signal-to-noise ratio for natural images," *IEEE Trans. Image Process.*, vol. 16, no. 9, pp. 2284–2298, Sep. 2007.

[3] Z. Wang, E. P. Simoncelli, and A. C. Bovik, "Multi-scale structural similarity for image quality assessment," in *Proc. IEEE Asilomar Conf. Signals, Syst. Comput.*, Nov. 2003, pp. 1398–1402.

[4] H. R. Sheikh, A. C. Bovik, and G. de Veciana, "An information fidelitycriterion for image quality assessment using natural scene statistics," *IEEE Trans. Image Process.*, vol. 14, no. 12, pp. 2117–2128, Dec. 2005.

[5] H. R. Sheikh and A. C. Bovik, "Image information and visual quality," *IEEE Trans. Image Process.*, vol. 15, no. 2, pp. 430–444, Feb. 2006.

[6] L. Zhang, L. Zhang, X. Mou, and D. Zhang, "FSIM: A feature similarity index for image quality assessment," *IEEE Trans. Image Process.*, vol. 20, no. 12, pp. 2378–2386, Aug. 2011.

[7] L. Zhang, L. Zhang, X. Mou, and D. Zhang, "A comprehensive evaluation of full reference image quality assessment algorithms," in *Proc. ICIP*, 2012.

[8] P. Perona and J. Malik, Scale Space and Edge Detection Using Anisotropic Diffusion Dept. of EECS Technical Report, University of California, Berkeley, 1988.

[9] A. Liu, W. Lin, and M. Narwaria, "Image quality assessment based on gradient similarity," *IEEE Trans. Image Process.*, vol. 21, no. 4, pp. 1500–1512, Apr. 2012.

[10] J. Zhu and N. Wang, "Image quality assessment by visual gradient similarity," *IEEE Trans. Image Process.*, vol. 21, no. 3, pp. 919–932, Mar. 2012.

[11] N. Ponomarenko, V. Lukin, A. Zelensky, K. Egiazarian, M. Carli, and F. Battisti, "TID2008—A database for evaluation of full-reference visual quality assessment metrics," *Adv. Modern Radioelectron.*, vol. 10, pp. 30–45, 2009.

[12] C. Larson and D. M. Chandler, Categorical Image Quality (CSIQ) Database 2009 [Online]. Available: http://vision.okstate.edu/csiq

[13] H. R. Sheikh, K. Seshadrinathan, A. K. Moorthy, Z. Wang, A. C. Bovik, and L. K. Cormack, Image and Video Quality Assessment Research at LIVE 2004 [Online]. Available: http://live.ece.utexas.edu/research/quality

[14] A. Ninassi, P. Le Callet, and F. Autrusseau, Subjective Quality Assessment IVC Database 2005 [Online]. Available: http://www2.irccyn.ec-nantes.fr/ivcdb

[15] Y. Horita, K. Shibata, Y. Kawayoke, and Z. M. P. Sazzad, MICT: Image Quality Evaluation Database 2000 [Online]. Available: http://mict.eng.u-toyama.ac.jp/mict/index2.html

[16] D. M. Chandler and S. S. Hemami, A57 Database 2007 [Online]. Available: http://foulard.ece.cornell.edu/dmc27/vsnr/vsnr.html

[17] Z. Wang and Q. Li, "Information content weighting for perceptual image quality assessment," *IEEE Trans. Image Process.*, vol. 20, no. 5, pp. 1185–1198, May 2011.

[18] VQEG, Final Report From the Video Quality Experts Group on the Validation of Objective Models of Video Quality Assessment Apr. 2000 [Online]. Available: http://www.vqeg.org/

[19] R. Jain, R. Kasturi, and B. G. Schunck, *Machine Vision*. New York: McGraw-Hill, 1995.

[20] B. Jähne, H. Haubecker, and P. Geibler, *Handbook of Computer Vision and Applications*. New York: Academic, 1999.